Eur Biophys J (2005) 34: 91–96
DOI 10.1007/s00249-004-0430-3

ARTICLE

Harald Janovjak · Jens Struckmeier · Daniel J. Müller

Hydrodynamic effects in fast AFM single-molecule force measurements

Received: 1 April 2004 / Revised: 3 June 2004 / Accepted: 16 June 2004 / Published online: 15 July 2004

Abstract Atomic force microscopy (AFM) allows the critical forces that unfold single proteins and rupture individual receptor–ligand bonds to be measured. To derive the shape of the energy landscape, the dynamic strength of the system is probed at different force loading rates. This is usually achieved by varying the pulling speed between a few nm/s and a few μm/s, although for a more complete investigation of the kinetic properties higher speeds are desirable. Above 10 μm/s, the hydrodynamic drag force acting on the AFM cantilever reaches the same order of magnitude as the molecular forces. This has limited the maximum pulling speed in AFM single-molecule force spectroscopy experiments. Here, we present an approach for considering these hydrodynamic effects, thereby allowing a correct evaluation of AFM force measurements recorded over an extended range of pulling speeds (and thus loading rates). To support and illustrate our theoretical considerations, we experimentally evaluated the mechanical unfolding of a multi-domain protein recorded at 30 μm/s pulling speed.

Keywords Atomic force microscopy · Loading rates · Drag force · Dynamic force spectroscopy · Ig27-8

Abbrevations AFM: atomic force micrcoscopy · pN: piconewton · BR: bacteriorhodopsin · DFS: dynamic force spectroscopy · Ig27: immunoglobulin 27 · If27-8: immunoglobulin 27 octameric construct · BFP: biomembrane force probe

H. Janovjak · D. J. Müller (✉)
BioTechnological Center, University of Technology Dresden, 01307 Dresden, Germany

J. Struckmeier
Veeco Metrology, Digital Instruments, Santa Barbara, CA 93117, USA

D. J. Müller
Max-Planck-Institute of Molecular Cell Biology and Genetics, Pfotenhauerstr. 108, 01307 Dresden, Germany
E-mail: mueller@mpi-cbg.de
Tel.: +49-351-46340330
Fax: +49-351-46340342

Introduction

Since its invention by Binnig, Quate and Gerber in 1986, the atomic force microscope has proven to be an excellent tool for imaging a wide class of biological samples such as cells, nucleic acids and proteins (Czajkowsky et al. 2000; Müller et al. 2002a). More recently, the micromachined cantilever of the AFM has been employed to measure the forces that stabilize single proteins and form molecular bonds at the piconewton (pN) scale (Lee et al. 1994; Moy et al. 1994; Rief et al. 1997, 1998; Fritz et al. 1998). To this end, a single protein or ligand–receptor pair is tethered between the tip of the cantilever and a supporting sample surface (Fig. 1). The tip–sample separation is then continuously increased by displacing the surface at constant speed with a piezoelectric actuator. Plotting force (as derived by the deflection of the cantilever and Hooke's law) against the tip–surface separation then yields a force–extension spectrum that is characteristic of the molecule being studied.

In their initial experiments, Rief and coworkers applied single-molecule force spectroscopy to the muscle protein titin, which consists of repeats of globular immunoglobulin and tenascin domains (Rief et al. 1997, 1998). The continuous extension of the protein resulted in the subsequent unfolding of the globular domains, while the force necessary for the unfolding of each domain was revealed from the force spectrum. In contrast to most other unfolding experiments on globular proteins, the combination of single-molecule imaging and force spectroscopy yielded surprisingly detailed insight into inter- and intramolecular interactions of the membrane protein bacteriorhodopsin (BR) (Oesterhelt et al. 2000). It has been shown that structural elements of BR unfold sequentially and that their stability depends on the physiological environment of the protein (Müller et al. 2002b; Janovjak et al. 2003).

Recently, dynamic force spectroscopy (DFS) experiments have provided insights into the energy landscapes

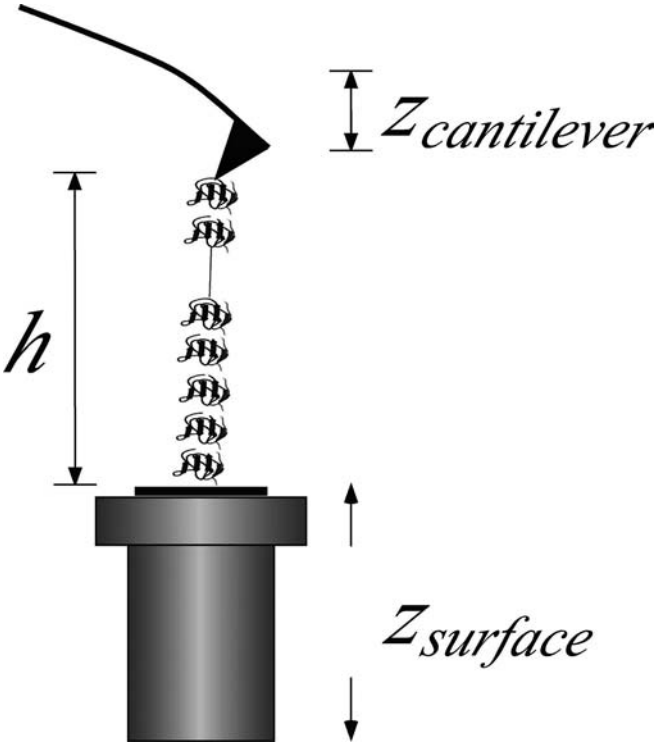

Fig. 1 Single-molecule force measurement on a multi-domain protein. A single multimeric protein construct consisting of several Ig27 domains is tethered between the AFM cantilever and a sample surface. Continuously increasing the tip–surface separation (h) by retracting the surface by $z_{surface}$ leads to unfolding of the individual domains. Measuring the deflection of the cantilever ($z_{cantilever}$) allows the force applied to the protein and thus required to unfold the single domains to be derived (Fig. 3)

underlying the mechanical properties of single biological molecules (Strunz et al. 1999; Evans 2001; Williams et al. 2003). In DFS, unfolding or unbinding forces are measured at various pulling speeds. Monitoring the most probable unbinding force as a function of pulling speed allows the width of potential barriers crossed during the unfolding process and the natural transition rates over these barriers to be revealed (Evans and Ritchie 1997; Evans 2001). In the case of Ig27 domains and single transmembrane helices of BR, it was found that a ≈4-Å extension triggers unfolding across a single potential barrier (Rief et al. 1997; Williams et al. 2003; Janovjak et al. 2004). Merkel and coworkers demonstrated that during unbinding of biotin from (strept-)avidin several potential barriers are crossed. Their positions along the separation distance could be localized using DFS without comparable spatial resolution of the instrument (Merkel et al. 1999).

All recent DFS experiments with AFM had in common that the pulling speeds were varied in the range from a few nm/s to ≈10 μm/s (de Paris et al. 2000; Williams et al. 2003). However, to obtain a more complete picture of their kinetic properties, it would be desirable to investigate the systems over an increased range of pulling speeds (Lo et al. 2001). At speeds greater than ≈10 μm/s, the speed-dependent hydrodynamic drag force acting on the cantilever is of the same magnitude as the peak forces measured on single biological molecules. As the tip velocity is not constant during typical measurements, large deviations in the forces are obtained if the hydrodynamic effects are not considered. This effect appears most significant at pulling speeds above a few μm/s. Here, we combined hydrodynamic force measurements and theoretical considerations to provide a method for the correct evaluation of force measurements recorded at pulling speeds, and hence loading rates, up to two orders of magnitude higher than previously possible.

Materials and methods

Atomic force microscopy

A commercial atomic force microscope (AFM) optimized for force measurements (MultiMode PicoForce, Veeco Metrology, Santa Barbara, CA) was equipped with a x-y-z-piezo scanner with a sensored and closed-loop 20-μm z-axis. The spring constants of the two silicon nitride cantilevers (small V-shaped lever: Olympus OTR4, $k = 0.095$ N/m, length (l) = 100 μm, width (w) = 18 μm, thickness (t) = 0.4 μm; large V-shaped lever: ThermoMicroscope MSCT-AUNM Microlever C, $k = 0.015$ N/m, $l = 320$ μm, $w = 22$ μm, $t = 0.6$ μm; Veeco Metrology) were calibrated in liquid using thermal fluctuation analysis (Butt and Jaschke 1995; Florin et al. 1995).

Experimental unfolding data on Ig27-8

Individual molecules were unfolded as recently described (Rief et al. 1997) using the large V-shaped lever in PBS (Sigma) after adsorption to a freshly prepared gold surface. We used the worm-like chain model with a persistence length of 4 Å and a monomer length of 3.6 Å to describe the force–extension relationship of unfolded parts of the protein in the force spectrum (Rief et al. 1997).

Results and discussion

Hydrodynamic drag force acting on an AFM cantilever

Like any other object moved through a solution, the AFM cantilever experiences a hydrodynamic drag force due to viscous friction with the surrounding liquid (Walters et al. 1996; Gittes and Schmidt 1998; Viani et al. 1999a). Drag forces have been previously quantified for spheres as well as for an AFM cantilever close to a surface (Cox and Brenner 1967; Alcaraz et al. 2002). For a cantilever, it has been suggested that the dimensions of the lever and the distance to the surface be scaled by introducing two empirical coefficients (Roters and Johannsmann 1996; O'Shea and Welland

1998; Alcaraz et al. 2002). As recently proposed, the drag force (F_d) acting on the cantilever can then be described as:

$$F_d = \frac{6\ \pi\ \eta a_{eff}^2}{h + d_{eff}} \cdot v_{tip} \quad (1)$$

where η is the viscosity of the liquid, h the tip–surface separation and v_{tip} denotes the tip velocity (Alcaraz et al. 2002). The empirical coefficients a_{eff} and d_{eff} represent the effective size of the cantilever and the effective cantilever tip height respectively. Equation (1) is valid in regimes of purely viscous flow, i.e. where the Reynolds number ($Re = a_{eff} v_{tip} \rho / \eta$) is below 1 (Alcaraz et al. 2002). For a typical measurement in water at room temperature ($\eta = 1$ mNs/m^2, density $\rho = 1$ g/cm^3), Re is well below 1 for pulling speeds as high as a few mm/s. We quantified the hydrodynamic drag force as a function of the pulling speed and tip–sample separation for two V-shaped cantilevers. Figure 2a shows the linear dependence of the drag force on the pulling speed, and Fig. 2b the more complex dependence on the tip–surface separation. As predicted, an increase in the drag force is observed close to the surface (Roters and Johannsmann 1996). Consequently, a_{eff} and d_{eff} were determined by measuring the drag force at a fixed speed for different tip–sample separations and fitting the data to Eq. (1). For a_{eff} we obtained 35.13 ± 0.07 µm (small lever) and 52.06 ± 0.08 µm (large lever), and for d_{eff} 3.70 ± 0.18 µm (small lever) and 5.48 ± 0.17 µm (large lever). Although the above model predicts $F_d = 0$ for large separations (Alcaraz et al. 2002), it accurately describes the drag force for a range of tip–sample separations sufficient for single-molecule force measurements (0–2.5 µm, Fig. 2b).

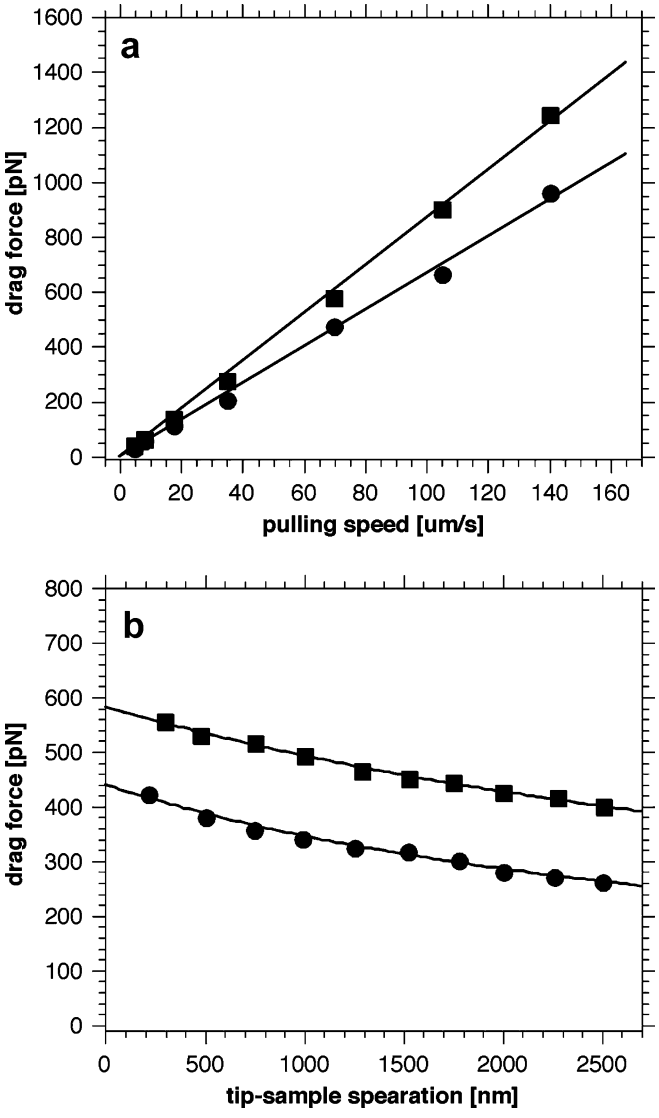

Fig. 2a, b Hydrodynamic drag force acting on an AFM cantilever. Force measurements with AFM cantilevers are subject to hydrodynamic drag forces, which depend on the pulling speed and tip–sample separation. **a** Linear dependence of the drag force on the pulling speed recorded at a distance of 500 nm from the surface. Slopes of the linear fits are 8.68 ± 0.11 pN s/µm (*squares*, large lever in PBS) and 6.67 ± 0.11 pN s/µm (*circles*, small lever in water). **b** Non-linear dependence of drag force on the tip–sample separation (recorded at 70 µm/s) which allows the empirical drag coefficients a_{eff} and d_{eff} to be determined according to Eq. (1) (*solid lines*). SDs are of comparable size with the markers

Correcting AFM force measurements for hydrodynamic effects

The hydrodynamic force has to be considered in force measurements with pulling speeds above a few µm/s as it reaches the same magnitude (Fig. 2a) as the forces measured on single molecules (Lee et al. 1994; Moy et al. 1994; Rief et al. 1997, 1998; Fritz et al. 1998). Including a correction factor for the hydrodynamic drag is complicated by the fact that the tip velocity is not constant during a typical measurement. Bending of the cantilever towards the surface is observed in most experiments when the cantilever is connected to the surface via a flexible linker molecule (e.g. polymer spacers for the study of single ligand-receptor pairs or already unfolded domains in case of proteins) (Rief et al. 1997; Hinterdorfer et al. 2000). Thus a direct consequence of any adhesive event is that the tip velocity decreases. In these cases, the tip–surface separation can be written as:

$$h = z_{surface} - z_{cantilever} \quad (2)$$

where $z_{surface}$ is the distance the surface has moved, and $z_{cantilever}$ is the cantilever deflection (Fig. 1). The tip velocity can then be calculated by taking the derivative of the tip–sample separation with respect to time for each point of the curve:

$$v_{tip} = \frac{dh}{dt} \quad (3)$$

As the tip velocity decreases during the measurement, the hydrodynamic drag force acting on the cantilever will also decrease. Therefore, the real force applied to the molecule is underestimated (i.e. it is larger than the

measured force) if hydrodynamic effects are not considered. This additional hidden force (ΔF) can be written as

$$\Delta F = F_{\mathrm{d}}(v,h) - F_{\mathrm{d}}(v_{\mathrm{tip}},h) \quad (4)$$

It is equal to the difference between the drag force calculated for the constant speed of the surface, $F_{\mathrm{d}}(v,h)$, and the drag force calculated by taking the tip velocity at each point of the curve into account, $F_{\mathrm{d}}(v_{\mathrm{tip}},h)$. Accordingly, the net force (F_{net}) acting on the molecule is:

$$F_{\mathrm{net}} = F_{\mathrm{measured}} + \Delta F \quad (5)$$

where F_{measured} is the measured force data. Equation (5) is valid if the offset of the unprocessed data is corrected by moving the non-contact part of the curve to zero force.

Unfolding a multi-domain protein at 30 μm/s

We observed the predicted underestimation during the unfolding of an octameric immunoglobulin-27 protein construct (Ig27-8) at 29.7 μm/s (Fig. 3a, solid line). The continuous extension of the multi-domain protein led to sequential unfolding of the domains, and thus the curve shows the characteristic sawtooth pattern (Rief et al. 1997; Fig. 3a, solid line). We measured an average unfolding force of 207.8 ± 35 pN ($n = 25$) for the unfolding of single Ig27 domains. However a force of ≈250 pN would be expected at this pulling speed when one extends the experimentally determined speed dependence of the unfolding forces to 30 μm/s (Williams et al. 2003).

To attribute this disagreement to the hydrodynamic effect described above, we inspected the tip–sample separation (Fig. 4a) and the tip velocity (Fig. 4b) in the course of the measurement. The tip–sample separation was derived according to Eq. (2), and each of the seven force peaks led to a local deviation from the linear behavior (Fig. 4a, arrows). Remarkably, the tip velocity (Fig. 4b, solid line) was not constant during the force curve and differed significantly from the speed with which the surface was separated from the cantilever (Fig. 4b, dashed line). As mentioned above, the tip moved more slowly when the cantilever was bent towards the surface. From the tip velocity we calculated the hydrodynamic drag force acting on the cantilever according to Eq. (1) (Fig. 4c). The observed decrease in the drag force indicates that the molecule was subjected to a hidden force in addition to the measured force. The re-evaluation of the curve following Eq. (5) is shown in Fig. 3, where the dashed line corresponds to the corrected force trace. It becomes clear that consideration of the hydrodynamic drag increases the peak forces significantly. After the correction, the measured unfolding force of a single Ig27 domain was 274.7 ± 37.5 pN ($n = 25$). As this value lies within the expected range it is suggested that correcting for the hydrodynamic drag allows a more correct evaluation of the measurement obtained at 29.7 μm/s.

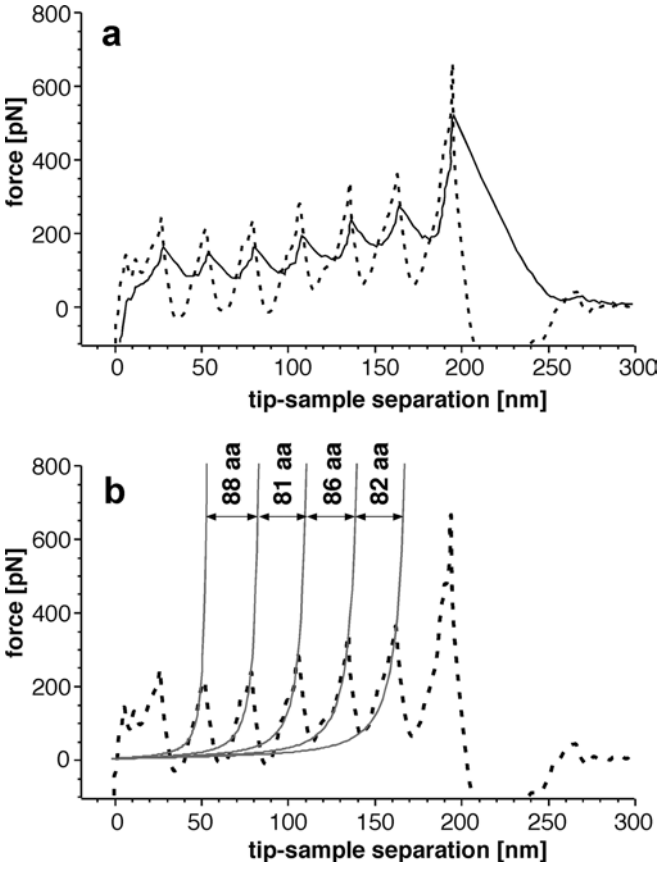

Fig. 3a, b Unfolding the multi-domain protein at 30 μm/s. **a** Plotting force as a function of tip–sample separation during the unfolding of the protein construct as shown in Fig. 1 yields the force extension curve (*solid line*). The sequential unfolding of the domains results in the characteristic sawtooth pattern. The *dashed line* corresponds to the same force trace after consideration of the hydrodynamic drag force. A significant increase in the peak forces by ≈50% is observed. **b** Fitting the corrected force trace with the WLC model indicates good agreement between the corrected experimental data and the expected extension pattern. The number of amino acid residues (*aa*) determined for each domain is given in the figure and is close to the length of the Ig27 domain (89 aa)

Factors limiting AFM pulling speeds

The apparent maximum instrumental pulling speed in AFM single-molecule force measurements is a few hundred μm/s (Lo et al. 2001). However, even after considering hydrodynamic contributions, the resonance frequency of the cantilever and its viscoelastic response time still limit AFM force measurements to lower pulling speeds. To ensure a proper response of the cantilever, the frequency of any repetitive feature in the force spectrum should be significantly lower than the resonance frequency of the cantilever (Viani et al. 1999a). When pulling Ig27-8 with a cantilever of 7-kHz resonance frequency (e.g. the small V-shaped lever), a speed of ≈100 μm/s is the limit, as this corresponds to

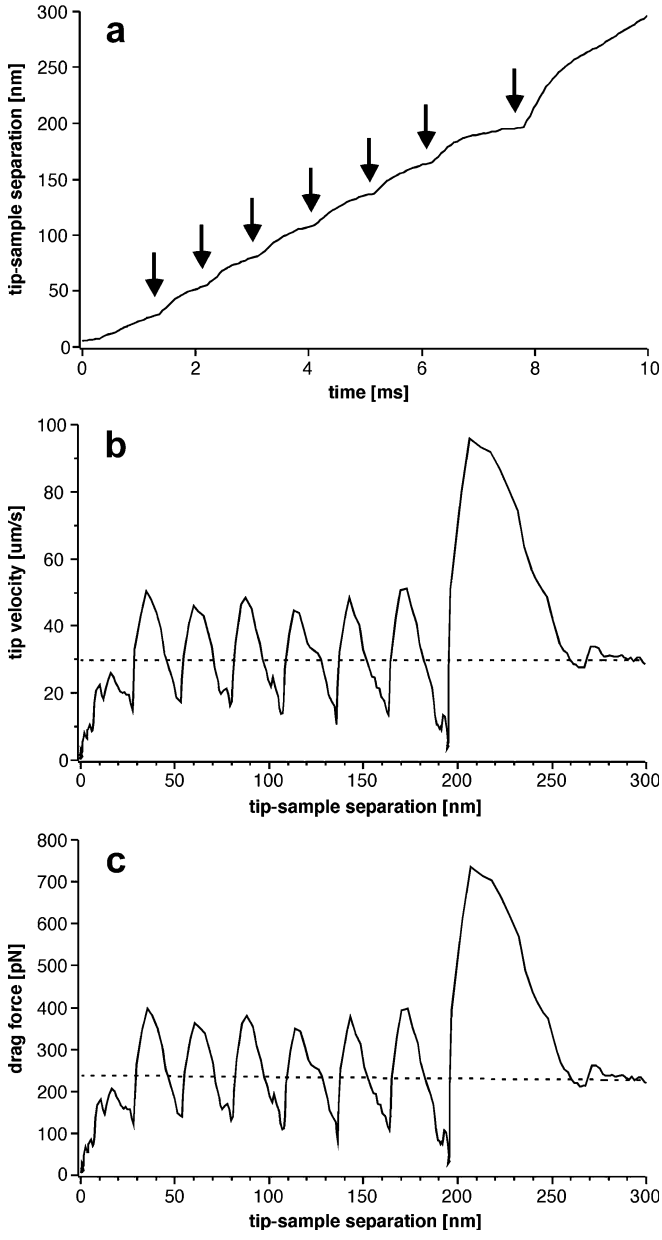

Fig. 4a–c Tip velocity and hydrodynamic drag force. **a** The separation of tip and sample during the measurement shown in Fig. 3a was derived following Eq. (2). A ridge in the linear curve is observed where the cantilever interacts with the surface (*arrows*). **b** The tip–sample separation was derived with respect to time according to Eq. (3) to obtain the velocity of the tip for each point of the force curve. As expected the tip moves more slowly when the cantilever interacts with the surface. **c** The hydrodynamic drag force acting on the tip of the cantilever was calculated for each point of the curve according to Eq. (1). The *dashed line* indicates the drag force for an untethered cantilever

a peak frequency in the force spectrum of ≈3 kHz. The viscoelastic response time of the cantilever is determined by the force probe's damping (Evans 2001). Assuming a probe damping (ζ) on the order of 10^{-3} pN s/nm and a spring constant (k) of 100 pN/nm, the time scale of viscoelastic responses ($t = \zeta/k$) lies in the range of 10^{-5} s (Evans 2001). This corresponds to a 'response frequency' of 100 kHz and thus to ≈30 responses per unfolding peak when unfolding Ig27-8 at 100 μm/s.

Comparison with ultra-small cantilevers

Such fast-pulling experiments could previously only be conducted with the help of ultra-small cantilevers (Viani et al. 1999a). Ultra-small cantilevers are typically ≈10–14 μm long, 3–5 μm wide and 100 nm thick (Viani et al. 1999b). The reduced cantilever size and mass result in smaller drag coefficients and higher resonance frequencies and thus allow access to higher pulling speeds. However, the use of such small cantilevers requires special instrumentation with a smaller laser spot size (Viani et al. 1999b). Furthermore, the production and handling of small cantilevers are challenging because, in order to obtain the same spring constant, the cantilever needs to be thinner than standard-size cantilevers (Viani et al. 1999a). It is important to note that our correction procedure is also suitable for extending the pulling speed range of small cantilevers.

Comparison with other force probe methods

Although many methods are in use, the AFM and the biomembrane force probe (BFP) may comprise the most frequently used techniques for measuring forces at a single-molecule level. The approach presented here allows a more complete investigation of the kinetic properties of the single molecule by AFM, as the range of accessible loading rates is extended. An extension becomes especially important because force measurements performed with the BFP are limited to loading rates of $\approx 10^5$ pN/s. This was estimated based on a maximum spring constant of 3 pN/nm and retraction speed of 20 μm/s (Merkel et al. 1999; Evans 2001). Faster retraction speeds may be difficult to achieve due to the temporal resolution of the optical detection systems and hydrodynamic contributions. As a loading rate of 10^5 pN/s corresponds to a pulling speed of 10 μm/s in AFM experiments (assuming a linker stiffness of 10 pN/nm) loading rates one to two orders of magnitude higher than with the BFP now become accessible with AFM.

Concluding remarks

In this article, we have shown that the tip velocity significantly decreases when an AFM cantilever interacts with a surface via a polymeric linker (Fig. 4b). To avoid an underestimation of the forces applied to the studied interaction, the hydrodynamic force acting on the cantilever has to be considered in measurements recorded at pulling speeds greater than a few μm/s (Fig. 3a). The

approach presented here allows an estimation of the hydrodynamic contributions and therefore extends the range of pulling speeds for all types of cantilevers used in AFM force measurements. This allows a more complete investigation of the kinetic properties as the dynamic range of bond strengths probed is currently limited primarily by the pulling speed.

Acknowledgements The authors are grateful to Ben Ohler, Alexej Kedrov, Julio Fernandez for his kind gift of the Ig27-8 sample, Niels Anspach, Ingmar Riedel, Matthias Rief, K. Tanuj Sapra and Pierre-Henri Puech. This work was supported by the Volkswagen Stiftung, the Free State of Saxony, and the European Union.

References

Alcaraz J, Buscemi L, Puig de Morales M, Colchero J, Baro A, Navajas D (2002) Correction of microrheological measurements of soft samples with atomic force microscopy for the hydrodynamic drag on the cantilever. Langmuir 18:716–721

Butt HJ, Jaschke M (1995) Calculation of thermal noise in atomic force microscopy. Nanotechnology 6:1–7

Cox RG, Brenner H (1967) Slow motion of a sphere through a viscous fluid towards a plane surface: small gap widths including inertial effects. Chem Eng Sci 22:1753

Czajkowsky DM, Iwamoto H, Shao Z (2000) Atomic force microscopy in structural biology: from the subcellular to the submolecular. J Electron Microsc 49:395–406

de Paris R, Strunz T, Güntherodt HJ, Hegner M (2000) Force spectroscopy and dynamics of the biotin-avidin bond studied by scanning force microscopy. Single Mol 1:285–290

Evans E (2001) Probing the relation between force—lifetime—and chemistry in single molecular bonds. Annu Rev Biophys Biomol Struct 30:105–128

Evans E, Ritchie K (1997) Dynamic strength of molecular adhesion bonds. Biophys J 72:1541–1555

Florin EL, Rief M, Lehmann H, Ludwig M, Dornmair C, Moy VT, Gaub HE (1995) Sensing specific molecular interactions with the atomic force microscope. Biosensors Bioelectr 10:895–901

Fritz J, Katopodis AG, Kolbinger F, Anselmetti D (1998) Force-mediated kinetics of single P-selectin/ligand complexes observed by atomic force microscopy. Proc Natl Acad Sci USA 95:12283–12288

Gittes F, Schmidt CF (1998) Thermal noise limitations on micromechanical experiments. Eur Biophys J 27:75–81

Hinterdorfer P, Kienberger F, Raab A, Gruber HJ, Baumgartner W, Kada G, Riener C, Wielert-Badt S, Borken C, Schindler H (2000) Poly(ethylene glycol): an ideal spacer for molecular recognition force microscopy/spectroscopy. Single Mol 1:99–103

Janovjak H, Kessler M, Oesterhelt D, Gaub H, Muller DJ (2003) Unfolding pathways of native bacteriorhodopsin depend on temperature. EMBO J 22:5220–5229

Janovjak H, Struckmeier J, Hubain M, Kedrov A, Kessler M, Muller DJ (2004) Probing the energy landscape of the membrane protein bacteriorhodopsin. Structure (Camb) 12:871–879

Lee GU, Chrisey LA, Colton RJ (1994) Direct measurement of the forces between complementary strands of DNA. Science 266:771–773

Lo YS, Zhu YJ, Beebe TP (2001) Loading-rate dependence of individual ligand-receptor bond-rupture forces studied by atomic force microscopy. Langmuir 17:3741–3748

Merkel R, Nassoy P, Leung A, Ritchie K, Evans E (1999) Energy landscapes of receptor-ligand bonds explored with dynamic force spectroscopy. Nature 397:50–53

Moy VT, Florin EL, Gaub HE (1994) Intermolecular forces and energies between ligands and receptors. Science 266:257–259

Müller DJ, Janovjak H, Lehto T, Kuerschner L, Anderson K (2002a) Observing structure, function and assembly of single proteins by AFM. Prog Biophys Mol Biol 79:1–43

Müller DJ, Kessler M, Oesterhelt F, Möller C, Oesterhelt D, Gaub H (2002b) Stability of bacteriorhodopsin alpha-helices and loops analyzed by single-molecule force spectroscopy. Biophys J 83:3578–3588

O'Shea SJ, Welland ME (1998) Atomic force microscopy at solid-liquid interfaces. Langmuir 14:4186–4197

Oesterhelt F, Oesterhelt D, Pfeiffer M, Engel A, Gaub HE, Müller DJ (2000) Unfolding pathways of individual bacteriorhodopsins. Science 288:143–146

Rief M, Gautel M, Oesterhelt F, Fernandez JM, Gaub HE (1997) Reversible unfolding of individual titin immunoglobulin domains by AFM. Science 276:1109–1112

Rief M, Gautel M, Schemmel A, Gaub HE (1998) The mechanical stability of immunoglobulin and fibronectin III domains in the muscle protein titin measured by atomic force microscopy. Biophys J 75:3008–3014

Roters A, Johannsmann D (1996) Distance-dependent noise measurements in scanning force microscopy. J Phys Condens Matt 8:7561–7577

Strunz T, Oroszlan K, Schafer R, Guntherodt HJ (1999) Dynamic force spectroscopy of single DNA molecules. Proc Natl Acad Sci USA 96:11277–12782

Viani MB, Schaffer TE, Chand A, Rief M, Gaub HE, Hansma PK (1999a) Small cantilevers for force spectroscopy of single molecules. J Appl Phys 86:2258–2262

Viani MB, Schaffer TE, Paloczi GT, Pietrasanta LI, Smith BL, Thompson JB, Richter M, Rief M, Gaub HE, Plaxco KW, Cleland AN, Hansma HG, Hansma PK (1999b) Fast imaging and fast force spectroscopy of single biopolymers with a new atomic force microscope designed for small cantilevers. Rev Sci Instrum 70:4300–4303

Walters DA, Cleveland JP, Thomson NH, Hansma PK, Wendman MA, Gurley G, Elings V (1996) Short cantilevers for atomic force microscopy. Rev Sci Instrum 67:3583–3590

Williams PM, Fowler SB, Best RB, Toca-Herrera JL, Scott KA, Steward A, Clarke J (2003) Hidden complexity in the mechanical properties of titin. Nature 422:446–449